Materials Research Proceedings **6** (2018) 39-44 doi: http://dx.doi.org/10.21741/9781945291890-7

In-Situ Synchrotron X-Ray Diffraction Studies in the Chip Formation Zone During Orthogonal Metal Cutting

Jens Gibmeier[1,a *], Dominik Kiefer[1,b], Rafael Hofsaess[1] and Norbert Schell[2,c]

[1] Karlsruhe Institute of Technology (KIT), Institute for Applied Materials (IAM-WK), Engelbert-Arnold-Str. 4, 76131 Karlsruhe, Germany

[2] Institute of Materials Research, Helmholtz-Zentrum Geesthacht (HZG), Max-Planck-Str. 1, 21502 Geesthacht, Germany

[a]Jens.Gibmeier@kit.edu, [b]Dominik.Kiefer@kit.edu, [c]Norbert.Schell@hzg.de

Keywords: Dry Metal Cutting, Turning, In-Situ X-Ray Diffraction, Synchrotron Radiation

Abstract. In the field of metal cutting a very important parameter is the chip formation zone, where the workpiece, the cutting tool and the chip are in contact. The transient processes inside this zone decisively define the properties of the workpieces near surface zone, e.g. residual stress distribution or the local microstructure. With the development of a special designed turning device we established a methodology to gain insight into the chip formation zone of a workpiece during the turning process with high spatial and temporal resolution. Using the dedicated device we were able to access the strain evolution during a cutting process of aluminum alloy AW-5754 with a measuring rate of 10 Hz inside the chip formation zone.

Introduction

Surface integrity is an important factor for service behaviour of machined workpieces, which is influenced by the chosen cutting parameters and by the tool wear. In this regard the residual stresses, surface quality and the local microstructure are essential parameters for the assessment. For low carbon steels and aluminium alloys built-up edge (BUE) formation is often observed on the rake face of the cutting tool, in particular in the low cutting speed regime and for example in micro machining. Due to the BUE the effect of cutting is displaced from the initial cutting edge towards the cutting edge of the BUE. For the cutting tool the adhering stagnant layers are very important for the wear behaviour. We recently found that the BUE can act as a protective layer and can improve the wear behaviour and thus the tool lifetime. Further, we found that because of detoriation of the surface roughness due to partial breaking of particles off the BUE, surface texturing of the cutting tool can be used to stabilise the BUE [1]. However, the fundamental relationships for BUE formation are not well-understood. In particular these transient processes hamper the prediction of chip forming operations by means of finite element simulations. A valuable step towards an improved process comprehension and for the sustainable improvement of simulation models for proper process prediction can be made if one succeeds in gaining real time insights in chip forming processing using technical relevant machining parameters. A vital tool in this regard is the application of synchrotron X-ray diffraction to monitor the microstructure and strain evolution in the chip formation zone with high temporal resolution. Having knowledge of these highly time-dependent evolutions allow for both, gaining knowledge about the mechanisms during machining in this zone, like local strain formation and texture development, which can further be used to optimize cutting processes, and process simulation through direct validation of simulations with real-time data from local synchrotron X-ray diffraction experiments. Up to know, there have not been a lot of investigations in the field of chip formation mechanism and the complex thermo-mechanical processes during cutting. First

Materials Research Proceedings **6** (2018) 39-44 doi: http://dx.doi.org/10.21741/9781945291890-7

results in the field of in-situ cutting were presented by Uhlmann [2] and later by Brömmelhoff [3] analyzing the stress state, the local texture and the microstructure in the shear zone during orthogonal cutting. However, the temporal resolved data were recorded in the very low cutting speed regime, while the chosen process parameters are far from conventional used cutting parameters (e.g. cutting speed etc.)

Here, we report on the establishment of a methodology to get an insight into the chip-tool-workpiece contact zone with high spatial and temporal resolution for cutting conditions near to conventionally used cutting parameters for orthogonal cutting. Angular dispersive high energy synchrotron X-ray diffraction in transmission geometry was performed at beamline P07B@Petra III during turning of aluminium alloy Al-Mg3 (AW-5754) using a specially designed turning rig in the cutting speed regime between 36 - 200 mm/min, which are cutting conditions that are prone to BUE formation.

Experimental

Orthogonal cutting was realized on hollow cylindrical samples made of Al-Mg3 (AW-5754) with a wall thickness of 2 mm, see Fig. 1 for dimension, which were completely turned off using a turning device that was specifically designed for this purpose (see Fig. 2 left). The turning rig was adjusted in the synchrotron radiation beam at P07B@PETRAIII at the German Electron Synchrotron in Hamburg, Germany. The device was specifically built to investigate both, the built-up edges and the chip formation zone. Hence, the tool is mounted at a fixed position and the workpiece realizes the feed [4]. Using this set-up multiple experiments were performed with variations of the cutting speeds v_c. A full list of the turning geometries and parameters is given in Table 1 (experiments A-D). As cutting tool we used uncoated cemented carbide inserts with 6 wt.% Co. The hollow cylindrical sample is mounted on the turning lathe with the 50 mm shaft in a three-jaw chuck.

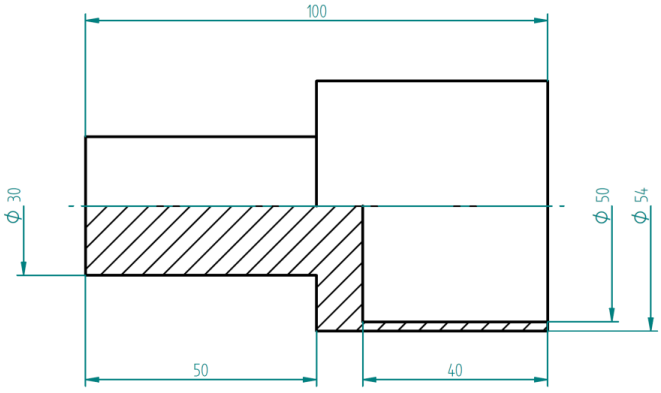

Fig. 1: Technical drawing of the hollow cylindrical sample with 2 mm wall thickness.

Table 1: Turning process angles and further cutting relevant parameters.

wall thickness t [mm]	2
cutting speed v_c[m/min]	(D)36;(A)150; (B) (C)200
feed rate v_f [mm/min]	25
feed length l_f [mm]	25
clearance angle α [°]	90
wedge angle β [°]	8
rake angle γ [°]	-8
entering angle κ [°]	45
indexable insert type	SNMA120408
clamp mounting type	PSSNR2020K15

The device was adjusted in the primary synchrotron radiation beam in such a way that the chip formation zone in the workpiece is irradiated at an inclination angle of 45° to the feed axis, see also Fig. 2. At P07B@Petra III a fixed photon energy of 87.1 keV (λ = 0.1425 Å) is provided by a single bounce monochromator (SBM). The beam size was set to 0.2 x 0.2 mm^2 for this first approach using a cross slit aperture, while the spot center was placed in a distance of 0.2 x 0.2 mm from the cutting edge towards the hollow cylindrical samples (Fig. 2 right). For diffraction pattern detection a 2D flat panel detector of type PerkinElmer XRD 1622 was used. By this means diffraction rings of the aluminum lattice planes {111}, {200}, {220} and {311}

Materials Research Proceedings **6** (2018) 39-44 doi: http://dx.doi.org/10.21741/9781945291890-7

were recorded with a measuring frequency of 10 Hz and were evaluated using the open-source software *Fit2D* [5].

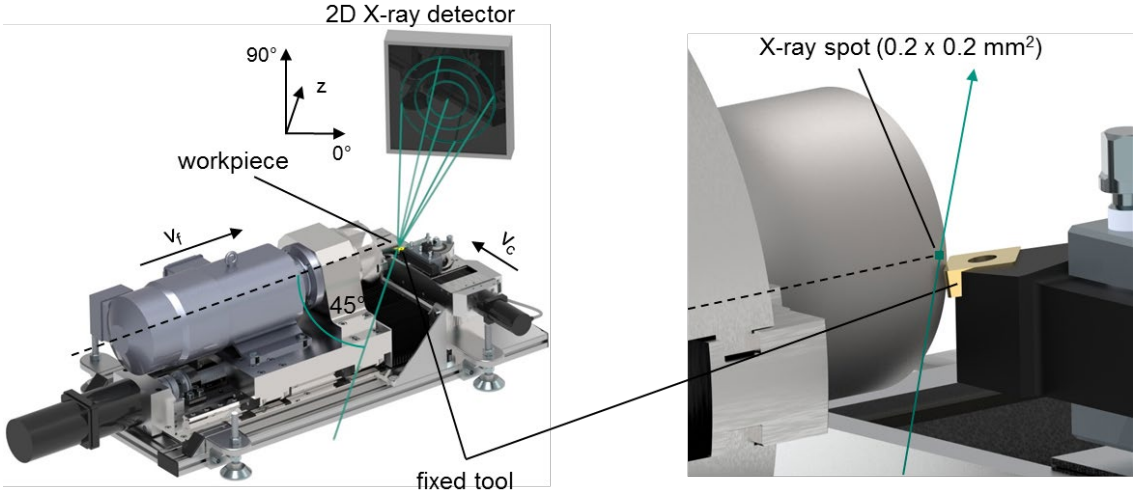

Fig. 2: (a) Experimental setup scheme with turning device and 2D PerkinElmer flat panel detector. (b) Detailed view on the irradiated process zone.

For the strain evolution analysis pie slices with an azimuthal angle range of 10° (± 5°) were defined and integrated for the 0° (normal to cutting plane) and 90° (parallel to cutting plane) direction (see Fig. 2 left and Fig. 3) to increase statistics. Thus, one dimensional intensity vs. 2θ datasets were determined that were further evaluated using a MATLAB script. Peak fitting was done using Pseudo-Voigt fit functions. From the calculated peak positions lattice spacings for the investigated interference lines were calculated on the basis of Bragg's law. The strain evolution for each direction (0° and 90°) was referenced to the first frame monitored; hence, strain changes were determined. The {hkl}-plane specific strain evolutions were averaged according to Daymond [6] using a texture coefficient of 1 for this first approach. The {hkl} specific elastic constants are calculated from single crystal elastic constants [7] using the Kröner model.

Results and Discussion

In Fig. 3 the extracted 1D diffraction profile is given for the 0° direction (experiment C) as an example. In the 2θ range of 2 to 8° the five measured Al diffraction lines are indexed. An analysis of the {222} Al diffraction plane was not performed due to the insufficient counting statistics. The relative intensities of the peaks do not show clear indication of texture or coarse grains, due to the fast rotating workpiece, which is in this investigation of great advantage. Due to the rotating workpiece always closely occupied diffraction rings were recorded. However, this blocks the possibility to monitor local texture evolution. Local texture can only by assessed for the final state, when the workpiece stops rotating.

In Fig. 4 and Fig. 5 the resulting strain evolution for the experiments A, B and C in normal (0°) and parallel (90°) direction to the cutting surface is plotted. In all cases the start of the cutting process is marked by a steep increase in tensile strains in a time period of approx. 5 s. The end of the cutting processes is reached when the feed ends and the strain evolution decreases exponentially. Investigation of the cutting inserts indicated that for all experiments presented here, built-up edges were formed, as intended by the choice of cutting parameters. We distinguished the experiments in ´stable´ (A, partially B) and ´instable´ (C, D) processes. Here, instable machining is characterized by vibrations due to a change in chip formation (i. e. type, conditions) resulting in a split up of the lattice strain courses in 0° direction.

Materials Research Proceedings **6** (2018) 39-44 doi: http://dx.doi.org/10.21741/9781945291890-7

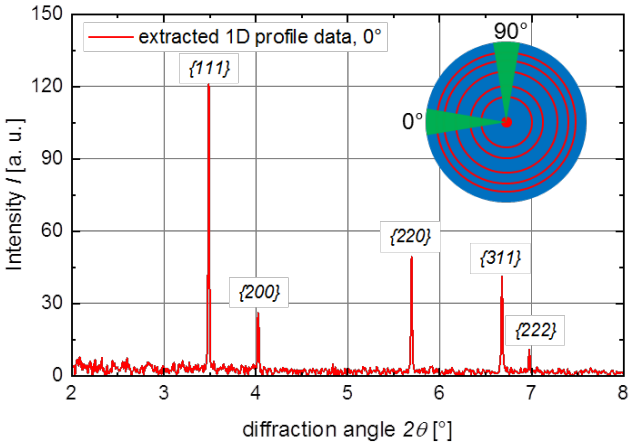

Fig. 3: Extracted 1D diffraction profile from monitored Debye-Scherrer rings of experiment C. Investigated lattice planes {hkl} are indexed.

In this regard, experiment A (Fig. 4 left) shows a stable cutting process, where a plateau is reached at about 10 s with 0.17 % strain for the average value. After approx. 60 s the average lattice strain falls in both directions to about 0.05 % residual strain after stop of processing. Experiment B starts analogously to A as a stable process with a plateau for the average strain of about 0.18 % in both directions. At about t = 55 s a steep rise of the lattice strain evolution in the normal and parallel direction can be observed (Fig. 4, Fig. 5 middle). Additionally a split up of the strain evolution between the evaluated reflections {hkl} in 0° direction can be noticed. This effect can be explained by a change in the cutting behavior. It is assumed that the formation of a built-up edge leads to a change in the chip shape geometry affecting the process stability due to a significant temperature increase leading to maximum average lattice strains of up to 0.45 %. In [4] a similar effect based on a steep temperature rise during the cutting of C45E was observed, which was due to a change in the chip shape geometry changing from spiral towards flow chips during continuous machining. Here, this significant temperature increase in the process zone lowers the warm yield strength of the workpiece resulting in higher plastic deformation, which is in correlation with the higher, residual lattice strain and the split up of lattice strain courses for the different {hkl} lines.

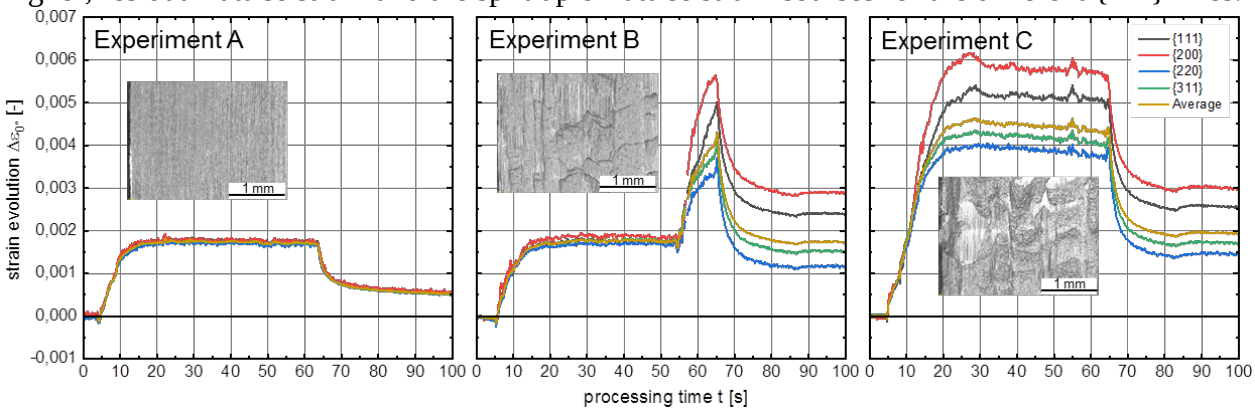

Fig. 4: Strain evolution vs. processing time for the investigated lattice planes and resulting average lattice strain according to [6] in 0° direction for experiments A (left), B (middle) and C (right). Micrographs of the cutting surfaces after the process are shown as thumbnails.

The increase in plastic deformation predominantly occurs in 0° direction, which is promoted by the larger constraint in this direction from the underlying material. The occurring differences in the lattice strain courses for different {hkl} planes are characteristic for fcc metals after plastic deformation and result due to plastic anisotropy through intergranular strains [8]. The split up of the lattice strain courses for different {hkl} lines is a clear indicator for the magnitude of plastic deformation induced during processing and in the present case much more meaningful as the peak widths of the recorded diffraction lines. The data indicate that experiment C (Fig. 4 and 5, right) depict an instable processing right from the start of the cutting.

Materials Research Proceedings **6** (2018) 39-44 doi: http://dx.doi.org/10.21741/9781945291890-7

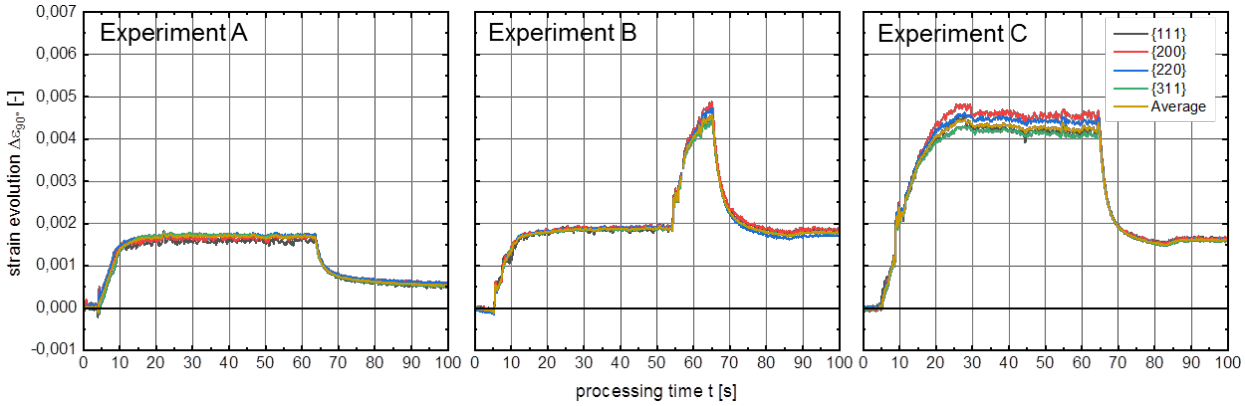

Fig. 5: Strain evolution vs. process time for the investigated lattice planes and resulting average lattice strain according to [6] in 90° direction for experiments A (left), B (middle) and C (right).

The upper average total strain plateau during the cutting is strongly increased to about 0.45 %. The reasons for this are the same as given for explanation of experiment B. It also can be seen, that the split of reflexes is, here again, only pronounced for the 0° direction. This is due to the higher strain restriction of the normal than to the parallel strain component by decreased temperature dissipation in the normal direction. The micrographs given in Fig. 4 show the workpiece surfaces after the process. In the stable case (experiment A) a homogeneous ground surface is depicted, whereas in the instable experiments B and C the cutting surface shows highly deformed areas confirming the higher plastic deformation in these cases.

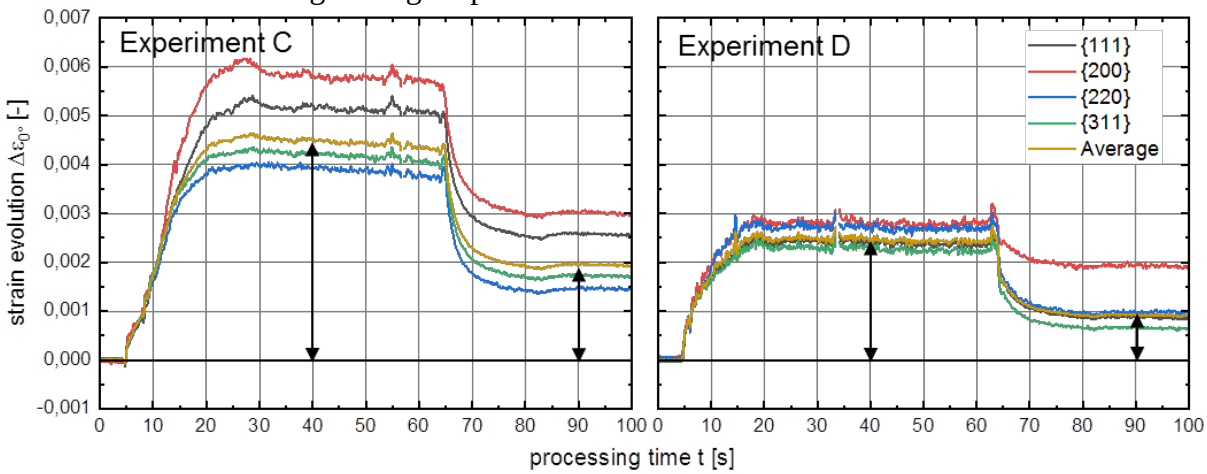

Fig. 6: Lattice strain evolution vs. process time for experiments C (left) and D (right). Arrows marking the averaged lattice strain differences during and after the cutting processes.

In Fig. 6 a direct comparison of experiments C and D is shown for the 0° direction, i.e. the strain component normal to the cut surface. Both processes show a split up of the lattice strain evolution, during and especially after cutting. It can be directly seen that the strain maximum during and after the processing as well as the degree of the split up is more pronounced for experiment C. In both cases the cutting is characterized by an instable processing leading to increased plastic deformation marked by the degree of split up between the lattice planes, especially for the {200} diffraction lines. For experiment C (v_c = 200 m/min) with increased cutting speed the average process induced lattice strain is about 0.2 % higher than for experiment D (v_c = 36 m/min) but the average residual lattice strain for B is about 0.2 % and for C about 0.1 %. The lower lattice strain differences in the final state (compared to the process) as well as the bigger split up in C indicate higher temperature in the process zone during cutting. This can

be explained by a larger decrease of the materials yield strength leading to a higher degree of plastic deformation compared to experiment D.

Summary

Real time monitoring of a turning process was successfully carried out using a special developed turning lathe and high energy synchrotron radiation. Thereby the lattice strain evolutions normal and parallel to the cutting surface inside the chip formation zone were investigated for orthogonal cutting using technical relevant cutting parameters of Al-Mg3 (AW-5754) with a measuring frequency of 10 Hz. From the experimental results determined for multiple diffraction lines {hkl} during machining conclusions of the quality of the machining process and the resulting surface can be derived.

The determined lattice strain evolutions clearly indicate changes in the cutting behavior and the chip shape geometry leading to instable cutting processes. The instability induces high temperature increases in the cutting zone, which cause significant plastic deformation especially in the direction normal to the cut surface. As a consequence a split up of the lattice strain courses for different {hkl} planes occurred, which are caused by plastic anisotropy through intergranular strains. The split up effect is a clear indicator for the degree of plastic deformation.

Acknowledgements

The authors gratefully acknowledge DESY for granting beamtime at P07B@PETRAIII and furthermore the technical support provided by DESY and HZG. The authors would also like to thank the WALTER AG for the provision of the cutting inserts.

References

[1] J. Kümmel, D. Braun, J. Gibmeier, J. Schneider, C. Greiner, V. Schulze, A. Wanner, Study on micro texturing of uncoated cemented carbide cutting tools for wear improvement and built-up edge stabilisation, J. Mat. Proc., 215 (2015), 62-70. https://doi.org/10.1016/j.jmatprotec.2014.07.032

[2] E. Uhlmann, R. Gerstenberger, S. Herter, T. Hoghé, W. Reimers, R. V. Martins, A. Schreyer, T. Fischer, In situ strain measurement in the chip formation zone during orthogonal cutting, Production Engineering, 5 1 (2011) 1-8. https://doi.org/10.1007/s11740-010-0266-x

[3] K. Brömmelhoff, S. Henze, R. Gerstenberger, T. Fischer, N. Schell, E. Uhlmann, W. Reimers, Space resolved microstructural characteristics in the chip formation zone of orthogonal cut C45E steel samples characterized by diffraction experiments, J. Mat. Proc., 213 8(2013) 2211-2216. https://doi.org/10.1016/j.jmatprotec.2013.06.016

[4] J. Kümmel, Detaillierte Analyse der Aufbauschneidenbildung bei der Trockenzerspanung von Stahl C45E mi t Berücksichtigung des Werkzeugverschleisses, Dissertation (2015).

[5] A. P. Hammersley, FIT2D: An Introduction and Overview, ESRF Internal Report ESRF97HA02T (1997).

[6] M. Daymond, The determination of a continuum mechanics equivalent elastic strain from the analysis of multiple diffraction peaks, J. Apl. Phys. 96 8 (2004) 4263-4272. https://doi.org/10.1063/1.1794896

[7] A. G. Every, A. K. McCurdy, Low Frequency Properties of Dielectric Crystals-Second and Higher Order Elastic Constants in: Landolt-Börnstein – Group III Condensed Matter, 29a, Springer Verlag, Heidelberg, (1992).

[9] A. J. Allen, M. Burke, W. I. F. David, S. Dawes, M. T. Hutchings, A. D. Krawitz, C. G. Windsor, Effects of Elastic Anisotropy on the Lattice Strains in Polycrystalline Metals and Composites Measured by Neutron Diffraction, ICRS 2 (1989) 78-83. https://doi.org/10.1007/978-94-009-1143-7_10